# Probabilistic Assessment of PV Hosting Capacity Under Coordinated Voltage Regulation in Unbalanced Active Distribution Networks

**CHANGHEE HAN**[1], (Graduate Student Member, IEEE),
**DONGWON LEE**[1], (Student Member, IEEE), **SUNGYOON SONG**[2], (Member, IEEE),
**AND GILSOO JANG**[1], (Senior Member, IEEE)

[1]Department of Electrical Engineering, Korea University, Seoul 02841, South Korea
[2]Advanced Power Grid Research Center, Korea Electrotechnology Research Institute, Uiwang-si 16029, South Korea

Corresponding author: Gilsoo Jang (gjang@korea.ac.kr)

**ABSTRACT** The increasing penetration of photovoltaic (PV) generators has led to a shift of the operational policy of the distribution system operator (DSO) from passive to active intervention in distribution networks (DNs), where a centralized controller governs the operation of voltage regulation devices. However, the PV output uncertainty hinders the verification of the impact of PVs on DNs. Therefore, the hosting capacity (HC) analysis framework for PV penetration should reflect both the operational benefit of the DSO and the PV output uncertainty. Thus, in this study, a two-stage optimization-based framework is proposed to analyze the probabilistic HC for PV under active network management (ANM) of DNs. In the first stage, the optimal PV base capacity (PVBC) to maximize the sum of the HC for PVs is determined based on a heuristic optimization method; in the second stage, using the predefined load and PV output profile, the maximum available power generation curve for PVBC is calculated, and the maximum HC for PV is derived by the calibration of PVBC through a comparison with the actual PV generation profile curve. The proposed method considers the time-series-based load flow results, reflecting the time-scheduling strategy by the DSO. Moreover, the uncertain characteristics of PV output are stochastically considered using a Monte Carlo simulation-based repetitive calculation approach. Case studies were implemented using the modified IEEE-123 test system, and the simulation results provided a quantitative comparison of the effect of the probabilistic HC improvement on the utilization of controllable resources and the centralized ANM by the DSO.

**INDEX TERMS** Active network management, distribution system, hosting capacity, optimization, photovoltaic system, probabilistic analysis, smart inverter, soft open point, voltage regulation.

## I. INTRODUCTION

The global tendencies to achieve net-zero emissions have led to a significant transition of the energy generation portfolio. In this regard, the integration of photovoltaic (PV) generators in distribution networks (DNs) has been accelerated [1]. However, the high penetration of PV in DNs has various negative impacts on the reliability and stability of grid operation involving voltage rise and fluctuations, load unbalance, loss increase, etc. [2]. In particular, the intermittent characteristics of PV generators cause significant uncertainty

The associate editor coordinating the review of this manuscript and approving it for publication was Guangya Yang.

in DNs. Hence, there is a demand for distribution network operators (DSOs) to know the maximum hosting capacity (HC) of PV for making economic decisions in network planning [3]. The maximum HC is defined as the capacity of distributed generators (DGs) that can be installed as much as possible without upgrading the power system while satisfying various constraints including network reliability [4]. Currently, in most countries, system operators determine the maximum HC for distributed generators (DGs) with a certain ratio of substation capacity [4]. However, in practice, the maximum HC can be determined by various constraints such as overvoltage, thermal capacity of the cable, and voltage unbalance limit. Therefore, a procedure for determining

the HC should simultaneously include all of these constraints [5].

To alleviate voltage-related issues in the presence of PV, several solutions for DN have been proposed. The most classical method is to maintain the voltage at the secondary side of the transformer using an on-load tap changer (OLTC) or a step voltage regulator [6]. In addition, the application of D-STATCOM, dynamic voltage regulators, and smart PV inverters are based on continuous reactive power support [7]. Recently, the application of voltage source converters (VSCs) in DNs, called soft open points (SOPs), has been studied to enable continuous power flow control between adjacent feeders in DNs [8]. From the perspective of the DSO, the local operation of these controllable resources without coordination is inefficient because it cannot address other negative impacts, such as frequent tap changes, interactions between control units, and increasing losses under the excessive circulation of reactive power in DNs [9]. Hence, optimally coordinated management of control devices from the central controller is generally more attractive [10], [11]. In [12], [13], a practical cooperative control between smart PV inverter and OLTC was proposed in consideration of the reactive power capability of the smart inverter in the low voltage DN. An aggregative energy management strategy was proposed in [14] to reflect the grid service of electric vehicles under the PV output uncertainty.

In the process to estimate the HC for PVs, the impact of this active network management (ANM) should be closely considered. Furthermore, the quantitative impact on HC enhancement, which is different depending on the coordination of control devices, should be assessed.

In [15], the robust operation of the OLTC and static var compensator (SVC) to address the uncertainty of DGs was considered in the process of determining the maximum HC. Moreover, the impact on HC improvement using smart PV inverters or network reconfiguration was assessed in [16] and [17], respectively. Worst case-based analytical approach was applied to determine HC in [14]. However, in the above methodologies, the voltage unbalance of the DN was not considered. Furthermore, the worst case-based deterministic approaches with regard to HC could be conservative because the volatility of DGs was not considered, which leads to underestimation of HC.

Therefore, stochastic approaches for determining HC have been studied in [18]–[23]. The methodologies differ depending on which factors are the sources of randomness. The authors in [18] proposed a framework to calculate HC in a probabilistic manner from randomized locations and array size of PVs in general DNs, and they developed the idea in [19] to consider the sensitivity of the HC regarding the combination of control schemes in ANM. In [20] and [21], a method to estimate the impacts on HC enhancement was proposed under the local control of voltage regulators or centralized ANM schemes, respectively.

However, the studies in [18]–[21] are based on the source of randomness from the network topology, such as location,

penetration ratio, and array size of PV, whereas the PV uncertainty and load output over time are not considered. Regarding the yearly wind speed prediction, the stochastic assessment of HC in ANM was studied in [22], but focused only on wind turbine (WT)-based DGs. In [23], the uncertainty of PV and WT-based DGs was considered in the proposed risk assessment tool for estimating the probabilistic HC, but the process is based on the method of checking for constraint violations, not on the optimized framework.

Besides, recent studies focused on obtaining additional benefits by operating the DN for other purposes rather than simply maximizing HC [24], [25]. In [24], the author proposed the optimal allocation of battery energy storage systems (BESSs) considering the power unbalance and voltage rise, achieving additional effects on maximizing the HC for PVs. Considering the optimal operation of the DN to minimize ohmic losses and voltage deviation, a fast calculation method to determine the HC was proposed based on multiparametric programming in [25]. However, since these studies did not consider a single objective of maximizing HC, there can be trade-off between enhancing HC and other objectives.

Hence, in this study, a framework to estimate the maximum HC for PVs in unbalanced networks is proposed, considering coordinated optimal control of voltage regulation devices, including smart inverters (SIs), OLTCs, SVCs, and SOPs. In addition to these controllable devices, DSO can operate the DN in coordination with BESSs to improve the HC for PVs [24], [26], [27]. However, the application of BESSs is beyond the scope of the current study. The constraints considered involve over-voltages, voltage unbalance limits, thermal capacity of lines, and substation capacity. The framework is divided into two optimization problems. In the first stage, based on the predefined daily load profile and specified PV locations, the optimal base capacity combination of PVs to maximize the total installed capacity was calculated for each time step. Consequently, the representative base capacity of each PV was determined. In the next stage, using the daily PV generation profile and base capacity determined in the previous step, the maximum HC for each PV was calculated. It is worth noting that, in the time-series-based load flow analysis of the proposed process, the optimal dispatch of voltage regulation devices was considered to maximize the total HC for PVs.

The proposed framework can be extended to probabilistic analysis through the random parameterization of the daily profile of PV and load. The main potential contributions of this study are threefold:

- A framework to calculate the maximum HC for PV under the optimal cooperation of ANM, including a tap changer, reactive power compensator and power flow controller, is proposed by solving two-step optimization problems. In addition, the impact of enhancing the HC for PV through ANM was verified through a comparison with the existing local control scheme;
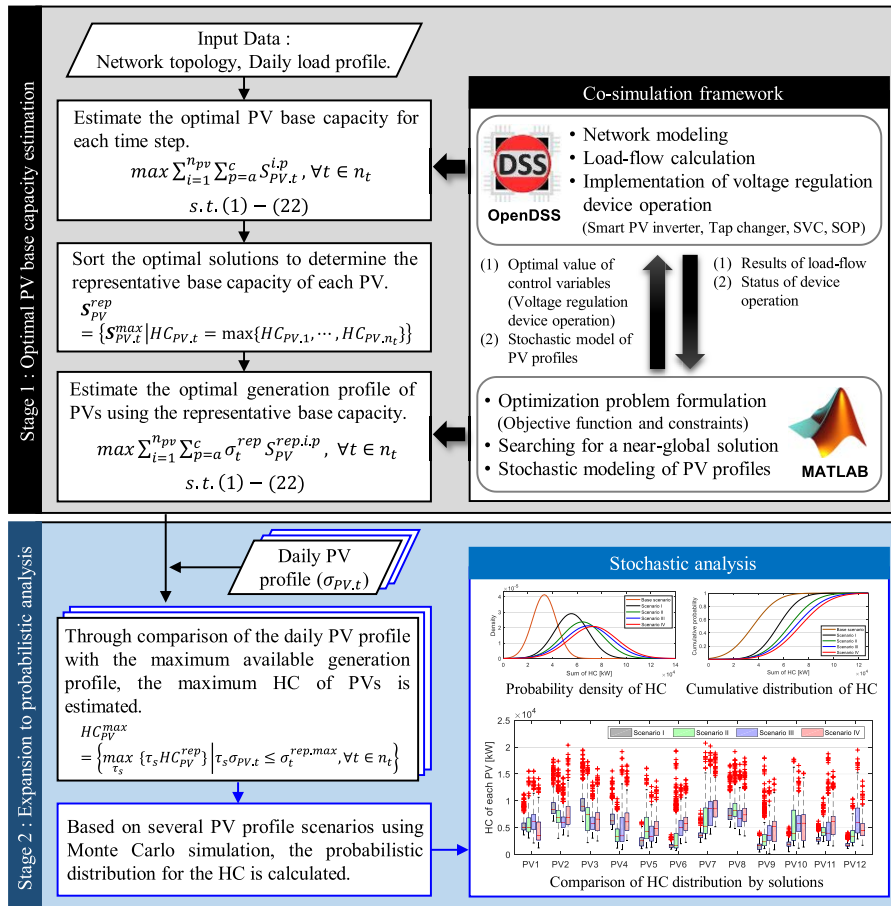
**FIGURE 1.** Proposed two-stage optimization framework for probabilistic HC assessment.

- Compared with previous studies, in which the location, array size, and number of PVs were considered as random variables, the uncertainty in PV and load output over time was considered to be random based on historical data. The DSO can calculate the HC information for the desired location of the PVs;
- The proposed process can be applied to both three-phase balanced and unbalanced DNs. Constraints limiting the maximum HC include overvoltage, voltage imbalance, and thermal capacity of lines and substations.

The remainder of this paper is organized as follows. Section II describes the entire two-stage optimization-based framework to determine the stochastic HC for the PV. Section III presents the simulation environments and discussion of the results of the case studies. Finally, the discussions and conclusions of this study are summarized in Section IV and V, respectively.

## II. TWO-STAGE OPTIMIZATION FRAMEWORK

The graphical procedure and flow chart of the proposed method are presented in Fig. 1. The proposed framework for estimating the maximum HC for PVs under the ANM scheme is divided into two stages. By formulating an optimization problem to maximize the total capacity of PVs with constraints in network reliability and operation of voltage regulation devices, the optimal base capacity of each PV is determined in the 1st stage. However, the maximum HC for PVs can differ depending on the shape of the daily PV generation profile curve. Therefore, in the 2nd stage, the maximum HC for a specific PV generation profile is determined through a comparison between the maximum available power generation profile and the actual PV generation profile. Further details are covered in Section II-C and D.

### A. CO-SIMULATION ENVIRONMENT

To solve the proposed optimization problems, a co-simulation environment is suggested using MATLAB with the open-source power flow tool, OpenDSS [28]. A network model with voltage regulation device operation (e.g., smart PV inverter, tap changer, SVC, and SOP) was implemented, and time-series-based load flow calculation was performed in OpenDSS. The proposed optimization problems were formulated in MATLAB to obtain the global solution. In this study, since the proposed objective function and logic-based constraints evaluated through OpenDSS are nonlinear and in the

form of black-box optimization, the genetic algorithm (GA) was used as a solver. GA is suitable for solving near-global optimization and is useful when performing co-simulation-based black-box optimization using two types of software. Other meta-heuristic optimization algorithms such as particle swarm or grey wolf optimization could be utilized according to the user's choice.

### B. PROBLEM FORMULATION

To implement the proposed optimization framework, the problems of the objective functions and constraints are formulated as follows:

#### 1) LOAD FLOW CONSTRAINTS

All node voltages and branch currents in the entire network are expressed using a nodal admittance matrix derived from Kirchhoff's current law as follows:

$$\boldsymbol{I}_{bus} = \boldsymbol{Y}_{system} \times \boldsymbol{V}_{bus} \qquad (1)$$

where $\boldsymbol{Y}_{system}$ is the branch admittance matrix of the entire network and has a matrix size of $3N \times 3N$ for three-phase modeling, in which $N$ is the number of buses in the DN. $\boldsymbol{I}_{bus}$ and $\boldsymbol{V}_{bus}$ are matrices of the branch current and nodal voltage, respectively. Finally, the power balance equations are generally derived as follows:

$$P^{i,p} = \sum_{j \in \Omega_{node.i}} \left| V^{i,p} \right| \left| V^{j,p} \right| \{ G^{ij,p} \cos \left( \theta^{ij,p} \right)$$
$$+ B^{ij,p} \sin \left( \theta^{ij,p} \right), \quad \forall i \in \Omega_{node}, \quad \forall p \in a, b, c \quad (2)$$

$$Q^{i,p} = \sum_{j \in \Omega_{node.i}} \left| V^{i,p} \right| \left| V^{j,p} \right| \{ G^{ij,p} \sin \left( \theta^{ij,p} \right)$$
$$- B^{ij,p} \cos \left( \theta^{ij,p} \right), \quad \forall i \in \Omega_{node}, \quad \forall p \in a, b, c \quad (3)$$

where $P^{i,p}$ and $Q^{i,p}$ are active/reactive power injections at $i$-th node in phase $p$, respectively. $V^{i,p}$ is single-phase complex voltage at $i$-th node in phase $p$. $G^{ij,p}$ and $B^{ij,p}$ represent the branch conductance and susceptance between $i$-th and $j$-th nodes in phase $p$, respectively. $\theta^{ij,p}$ is voltage angle difference between $i$-th and $j$-th nodes in phase $p$. $\Omega_{node.i}$ mean the set of nodes connected to the $i$-th node. $\Omega_{node}$ is the total node set in the network.

In this paper, load flow calculations in (1)–(3) are solved using an external tool (OpenDSS). Since OpenDSS is used in various studies related to power flow analysis and HC assessment [20], [29]–[31], the reliability of the power flow calculation results can be guaranteed.

#### 2) SMART PV INVERTER OPERATION

SIs connected with DGs have advanced control functions to offer ancillary services to the grid, such as voltage or frequency support [11], [12], [32], [33]. In this study, the impact of reactive power compensation capability in a PV-connected SI is considered in the process of determining the HC. Fig. 2 represents the volt-var droop curve of SIs, which can be
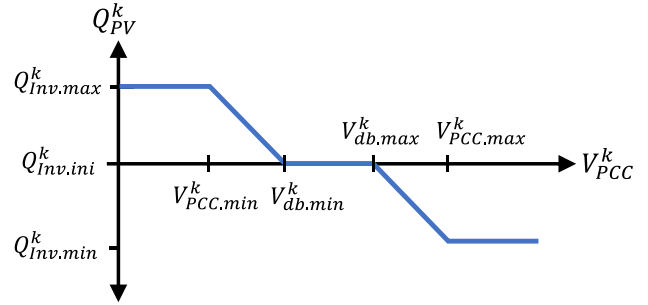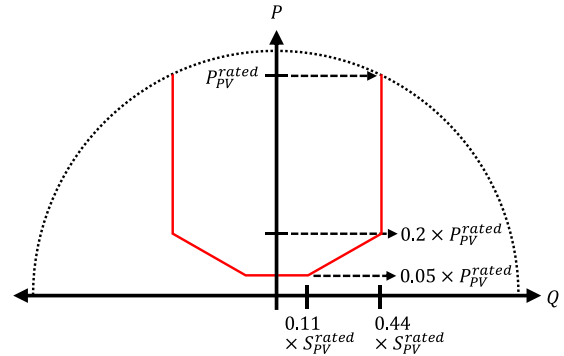
**FIGURE 2. Volt-var curve of the smart PV inverter.**

**FIGURE 3. Power capability of the smart PV inverter.**

generally formulated as in (4)–(8).

$$Q_{PV}^k \left( V_{PCC}^k \right)$$

$$= \begin{cases} Q_{Inv.max}^k, & \text{if } V_{PCC}^k \leq V_{PCC.min} \quad (4) \\ Q_{Inv.ini}^k, & \text{if } V_{db.min}^k \leq V_{PCC}^k \leq V_{db.max}^k \quad (5) \\ Q_{Inv.min}^k, & \text{if } V_{PCC}^k \geq V_{PCC.max} \quad (6) \\ \left( \dfrac{Q_{Inv.max}^k - Q_{Inv.ini}^k}{V_{PCC.min} - V_{db.min}^k} \right) \left( V_{PCC}^k - V_{db.min}^k \right) + Q_{Inv.ini}^k, \\ \qquad \text{if } V_{PCC.min} < V_{PCC}^k < V_{db.min}^k \quad (7) \\ \left( \dfrac{Q_{Inv.min}^k - Q_{Inv.ini}^k}{V_{PCC.max} - V_{db.max}^k} \right) \left( V_{PCC}^k - V_{db.max}^k \right) + Q_{Inv.ini}^k, \\ \qquad \text{if } V_{db.max}^k < V_{PCC}^k < V_{PCC.max} \quad (8) \end{cases}$$

$$Q_{PV.min}^{i,p} \leq Q_{PV.t}^{i,p} \leq Q_{PV.max}^{i,p} \qquad (9)$$

where $Q_{Inv.max}^k$, $Q_{Inv.min}^k$, and $Q_{Inv.ini}^k$ are the max/min bound and the initial reactive power outputs of the $k$-th SI, respectively. $V_{PCC}^k$ is the voltage magnitude at the connection point between the SI and the grid. The max/min value in the deadband range is defined using $V_{db.max}^k$ and $V_{db.min}^k$. $V_{PCC.max}$ and $V_{PCC.min}$ refer to the allowed upper/lower limits of the voltage at the connection point. This logic-based reactive power compensation can be simulated via OpenDSS [28].

The operating range of the SI with the PV is shown in Fig. 3, based on the IEEE Std. 1547-2018 [32]. According to [32], the curve parameters in Fig. 3 are defined by dividing them into two categories A and B regarding the penetration level of RESs in the power system. In this study, category B (high level of RES penetration) was applied. The reactive

power output limit in (9) is proportional to the apparent capacity of PVs, where $Q_{PV.t}^{i.p}$ represents the reactive power output of the smart PV inverter at time $t$ connected to the $i$-th node in phase $p$; the max/min reactive power capacities are defined as $Q_{PV.max}^{i.p}$ and $Q_{PV.min}^{i.p}$, respectively. If the owner of the PV generator uses an oversized inverter than the maximum power that can be transmitted through the PV panel, the reactive power output capability can be changed, however, these special cases were not considered in this paper. The parameters in the volt-var curve (i.e., slope or deadband of the curve) directly affect the HC for PVs [34]. In this study, the same parameters of the volt-var curve were applied to all PVs.

### 3) TAP CHANGER OPERATION
In the ANM framework, the tap position of the tap changing voltage regulator is directly dispatched from the DSO. If a transformer with a tap changer is installed between nodes $i$ and $j$ in phase $p$, the operation with tap limit constraints is modeled as (10)–(12).

$$V_{tap.t}^{i.p} = k_{tap.t}^{ij.p} V_{tap.t}^{j.p} \tag{10}$$

$$k_{tap.t}^{ij.p} = k_{tap.0}^{ij.p} + a_{tap}^{ij.p} N_{tap.t}^{ij.p} \tag{11}$$

$$N_{tap.min}^{ij.p} \leq N_{tap.t}^{ij.p} \leq N_{tap.max}^{ij.p} \tag{12}$$

where $k_{tap.t}^{ij.p}$ represents the tap ratio of the transformer at time $t$, and the initial ratio is $k_{tap.0}^{ij.p}$. The voltage adjustment ratio per tap step is defined as $a_{tap}^{ij.p}$. $N_{tap.t}^{ij.p}$ is the tap position at time $t$ with the lower and upper bounds of $N_{tap.min}^{ij.p}$ and $N_{tap.max}^{ij.p}$, respectively.

### 4) STATIC VAR COMPENSATOR OPERATION
The reactive power output of SVCs is also regarded as a control variable in the ANM framework, in which the constraints are expressed as:

$$\left| Q_{SVC.t}^{i.p} \right| \leq S_{SVC.rated}^{i.p} \tag{13}$$

where $Q_{SVC.t}^{i.p}$ is the reactive power output of the SVC at time $t$ in phase $p$, and $S_{SVC.rated}^{i.p}$ is the rated capacity of the SVC.

### 5) SOFT OPEN-POINT OPERATION
SOP is a set of two VSCs connected back-to-back to control the power flow. The active and reactive power outputs of SOPs can be independently regulated, and operating setpoints are considered as control variables in the ANM framework [8], as shown in (14)–(16).

$$\sum_{i=1}^{n_{sop}} \sum_{p=a}^{c} P_{SOP.t}^{i.p} + P_{loss.t}^{i.p} = 0 \tag{14}$$

$$P_{loss.t}^{i.p} = C_{loss}^{i.p} \sqrt{\left( P_{SOP.t}^{i.p} \right)^2 + \left( Q_{SOP.t}^{i.p} \right)^2} \tag{15}$$

$$\sqrt{\left( P_{SOP.t}^{i.p} \right)^2 + \left( Q_{SOP.t}^{i.p} \right)^2} \leq S_{SOP}^{i.p} \tag{16}$$

where $P_{SOP.t}^{i.p}$, $Q_{SOP.t}^{i.p}$, and $S_{SOP.t}^{i.p}$ refer to the active and reactive power outputs and rated capacity of the SOP, respectively. $n_{sop}$ is the number of VSCs consisting of the SOP. $C_{loss}^{i.p}$ is the device loss coefficient, for which a typical value of 0.02 is used [8]. Constraints (14) and (15) represent the power balance considering the device losses. The maximum capacity constraint is given by (16).

### 6) NETWORK RELIABILITY LIMITS
The node voltage magnitude limit is shown in (17):

$$V_{min} \leq \mathbf{V}_{n.t}^{i.p} \leq V_{max}, \quad \forall i \in \Omega_{node}, \quad \forall p \in \{a, b, c\} \tag{17}$$

where $\mathbf{V}_{n.t}^{i.p} = \left[ V_{n.t}^{i.a}, V_{n.t}^{i.b}, V_{n.t}^{i.c} \right]^{\mathrm{T}}$ represents the matrix of the node voltage at time $t$.

The node voltage unbalance limit is expressed as (18)–(20).

$$V_{avg.t}^i = \frac{1}{3}(V_{n.t}^{i.a} + V_{n.t}^{i.b} + V_{n.t}^{i.c}) \tag{18}$$

$$\mathbf{V}_{ub.t}^{i.p} = \left| \frac{\mathbf{V}_{n.t}^{i.p} - V_{avg.t}^i}{V_{avg.t}^i} \right| \tag{19}$$

$$\mathbf{V}_{ub.t}^{i.p} \leq V_{ub.max}, \quad \forall i \in \Omega_{node}, \quad \forall p \in \{a, b, c\} \tag{20}$$

where $\mathbf{V}_{ub.t}^{i.p} = \left[ V_{ub.t}^{i.a}, V_{ub.t}^{i.b}, V_{ub.t}^{i.c} \right]^{\mathrm{T}}$ means the voltage unbalance rate per phase $p$. ANSI C84.1 standard [35] suggests that the maximum deviation from the average voltage between the three phases should be less than 3%. Equations (21) and (22) represent the maximum capacity constraints of the power flow in the cable and substation, respectively:

$$\mathbf{S}_{br.t}^{j.p} \leq S_{br.max}^{Thr}, \quad \forall j \in \Omega_{br}, \quad \forall p \in \{a, b, c\} \tag{21}$$

$$S_{tr.t}^k \leq S_{tr.max}^{Thr}, \quad \forall k \in \Omega_{tr} \tag{22}$$

where $\mathbf{S}_{br.t}^{j.p} = \left[ S_{br.t}^{j.a}, S_{br.t}^{j.b}, S_{br.t}^{j.c} \right]^{\mathrm{T}}$ is the apparent power of the $j$-th branch at time $t$. $S_{tr.t}^k$ is the apparent power across the $k$-th substation transformer at time $t$. $\Omega_{br}$ and $\Omega_{tr}$ are the total set of branches and substation transformers in the entire network, respectively.

### C. OPTIMAL PV BASE CAPACITY ESTIMATION
In the proposed framework, two sequential optimization problems were formulated to determine the total HC for the PV. In the first optimization problem, considering the ANM operation and network reliability constraints which are modeled in the previous chapter, the optimal combination of each PV capacity at which the total sum of installed capacity of PVs is maximized is calculated every hour. The decision variables in the first optimization problem, which is expressed as (23), include the capacity of each PV at the predetermined location, tap position of the transformer, reactive power output of SVCs, and active/reactive power output of SOPs.

$$\max \quad \sum_{i=1}^{n_{pv}} \sum_{p=a}^{c} S_{PV.t}^{i.p}, \quad \forall t \in n_t$$
$$s.t. \quad (1) - (22) \tag{23}$$

where $\mathbf{S_{PV.t}} = \left[ S_{PV.t}^{1.a}, S_{PV.t}^{1.b}, S_{PV.t}^{1.c}, \cdots, S_{PV.t}^{n_{pv}.c} \right]^{\mathrm{T}}$ is the matrix of the PV capacity at time $t$ in phase $p$. $n_{pv}$ is the total

number of PVs. $n_t$ represents the entire time horizon of the proposed methodology.

In actual DNs, because the load profile over time is different for each type of load (e.g., residential, commercial, or industrial), the combination of each PV capacity to maximize the total HC can be different over time. Hence, the optimal PV base capacity (PVBC) is defined in (24) as the maximum PV capacity over time, which is calculated by solving the following optimization problem:

$$S_{PV.t}^{max} = \arg max(\sum_{i=1}^{n_{pv}} \sum_{p=a}^{c} S_{PV.t}^{i.p}) \tag{24}$$

where $S_{PV.t}^{max} = \left[ S_{PV.t}^{max.1.a}, S_{PV.t}^{max.1.b}, \cdots, S_{PV.t}^{max.n_{pv}.c} \right]^{\mathrm{T}}$ is the matrix of the PVBC at time $t$ in phase $p$. Therefore, the HC with PVBC over time can be defined as:

$$HC_{PV.t} = \sum_{i=1}^{n_{pv}} \sum_{p=a}^{c} S_{PV.t}^{max.i.p} \tag{25}$$

As the next step, the representative PVBC is defined as the PVBC at the maximum HC during the day, as shown in (26).

$$S_{PV}^{rep} = \left\{ S_{PV.t}^{max} \mid HC_{PV.t} = \max\{HC_{PV.1}, \cdots, HC_{PV.n_t}\} \right\} \tag{26}$$

where $S_{PV}^{rep} = \left[ S_{PV}^{rep.1.a}, S_{PV}^{rep.1.b}, \cdots, S_{PV}^{rep.n_{pv}.c} \right]^{\mathrm{T}}$ is the matrix of the representative PVBC capacity in phase $p$.

Based on the representative PVBC, a generation profile variable $\sigma_t^{rep}$ is defined as an index to calculate the amount of power generation possible for each time step during the entire time horizon. The second optimization problem is then formulated as (27) to estimate the maximum generation profile as in (28). The decision variables in (27) are the generation profile and operation state of the voltage regulators (i.e., operation setpoints of the tap changer, SVCs, and SOPs).

$$\max \quad \sum_{i=1}^{n_{pv}} \sum_{p=a}^{c} \sigma_t^{rep} S_{PV}^{rep.i.p}, \quad \forall t \in n_t$$
$$s.t. \quad (1)-(22) \tag{27}$$
$$\sigma^{rep.max} = \arg max(\sum_{i=1}^{n_{PV}} \sum_{p=a}^{c} \sigma_t^{rep} S_{PV}^{rep.i.p}) \tag{28}$$

where $\sigma^{rep.max} = \left[ \sigma_1^{rep.max}, \sigma_2^{rep.max}, \cdots, \sigma_{n_t}^{rep.max} \right]^{\mathrm{T}}$ is the matrix of maximum generation profile of the representative PVBC.

Among the solutions of (27), the optimal generation profile, which is expressed in (28), is the maximum available power generation ratio of the representative PVBC for each time step. Hence, if the representative PVBC is applied to a predetermined location, the maximum HC for PVs can be calculated through a comparison with the maximum generation profile during the entire time horizon with the actual PV profile curve. Note that there is one maximum HC for PVs per actual PV profile curve.

### D. EXPANSION TO PROBABILISTIC ANALYSIS
Through the process described in Section II-C, the representative PVBC is calculated for each load profile. The
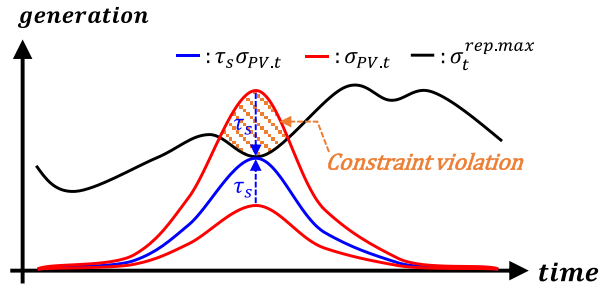


**FIGURE 4.** PV generation profile curve comparison.

maximum available generation profile is then defined as the generation profile of a representative PVBC that can be maximized within a value between 0% and 100% without violating network reliability constraints.

As shown in Fig. 4, when the representative PVBC actually produces electricity according to the PV generation profile for one day, the actual PV generation profile ($\sigma_{PV.t}$) can be greater than the maximum available generation profile ($\sigma_t^{rep.max}$) at a specific time. This means that in sections where the actual PV profile exceeded the maximum available generation profile, the network reliability constraints can be violated. Therefore, we proposed the correction variable ($\tau_s$) to adjust the scale of the actual PV profile curve by multiplying this until there was no cross section between the two curves. In contrast, no contact between the two curves indicates that PVs can generate more than the actual profile. Hence, the scale of the actual PV profile was maximized using the correction variable.

Finally, the maximum HC based on the representative PVBC can be calculated as shown in (29) by comparing the actual PV profile curve with the maximum available generation profile.

$$HC_{PV}^{max} = \left\{ \max\{\tau_s HC_{PV}^{rep}\} \mid \tau_s \sigma_{PV.t} \le \sigma_t^{rep.max}, \; \forall t \in n_t \right\} \tag{29}$$

where $HC_{PV}^{rep} = \sum_{i=1}^{n_{pv}} \sum_{p=a}^{c} S_{PV}^{rep.i.p}$ is the total sum of the representative PVBC. $\sigma_{PV.t}$ is the actual generation rate of PV over the entire time horizon. $\tau_s$ is the correction variable used to adjust the mismatch between the calculated maximum available generation profile and the actual PV profile.

Through the proposed process, one maximum HC for the PVs was calculated for each actual PV profile curve. In this study, based on historical data, numerous PV generation curves were generated during the analysis time horizon (one day) following the probability distribution of actual irradiance records. Then, the probabilistic HC for PVs was assessed through the repetition of the proposed method, reflecting the variability characteristic of PV. For example, if the HC distribution is calculated considering 50 load profiles and 100 PV generation profiles, the 50 maximum available generation profiles and the 100 corresponding correction variables are determined. The distribution for a total of $5,000(= 50 \times 100)$ HCs is then calculated. Note that the proposed method can consider the strategy of ANM in an unbalanced DN.
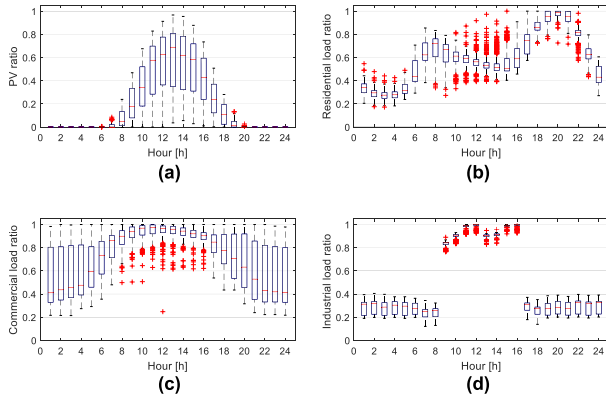
**FIGURE 5.** Probabilistic distribution of PV and each load types: (a) PV, (b) Residential load, (c) Commercial load, (d) Industrial load.

## III. CASE STUDIES

### A. UNCERTAINTY SCENARIO CONSTRUCTION

According to the proposed methodology, the source of the probability distribution in the HC for PVs comes from the variability of power output over time in PV and load demand. Therefore, a scenario construction is necessary for PV and load output over time, which can reflect their uncertainty. However, in this study, we focused on analyzing the stochastic HC for a given set of scenarios consisting of generation and load profiles. Thus, scenario generation techniques for modeling the uncertainty of PV or load are beyond the scope of this study.

Therefore, in this study, a scenario set for several daily generation and load profiles was constructed by utilizing the results of previous studies [36]–[38]. The process for determining the HC for PVs was repeatedly performed in a proposed two-stage optimization by randomly selecting these daily profiles in the scenario set based on a Monte Carlo method. Further, to simulate actual load variability, the load profiles are classified into three types: residential, industrial, and commercial. Each load type has different stochastic characteristics. Fig. 5 represents a box plot with 1-year historical data for PV output in a specific region [36] and load data for each type [37], [38].

### B. UNBALANCED TEST SYSTEM

To verify the proposed scheme in the unbalanced distribution system, a modified IEEE-123 test system was applied. The load ratings were not changed compared with the original test system [39]. The configuration of the modified test system is shown in Fig. 6 and assumes that three SVCs are installed in specific locations for cooperative voltage regulation with tap changers and smart PV inverters. Twelve PVs will be installed in specific locations. The classification of load types by location in the modified test system was referred to [40].

The specifications of the PVs, SVCs and SOPs in the test system are listed in Table 1. The locations of the single and three-phase PVs can be modified according to the intention of the DSO.
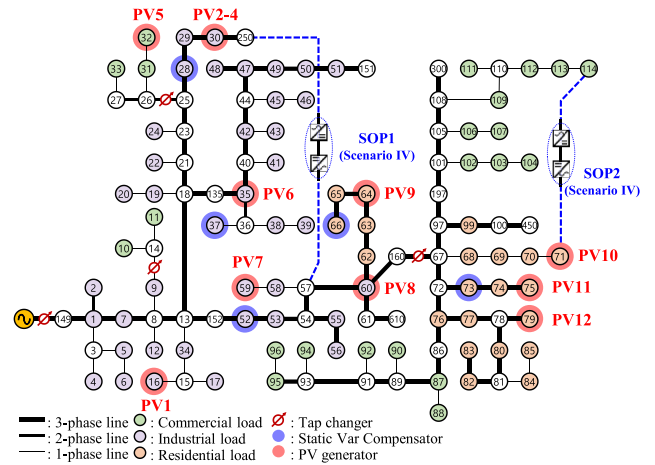


**FIGURE 6.** Configuration of unbalanced test network.

**TABLE 1.** Specifications of the test system.

| Resources | | Capacity [kVA] | Location [Bus number] | | |
|---|---|---|---|---|---|
| | | | Phase *a* | Phase *b* | Phase *c* |
| Single-phase | PV | - | 60, 71 | 59, 64, 79 | 16, 32, 35, 75 |
| | SVC | 2,000 | 28, 37 | - | 66, 73 |
| | SOP | 3,000 | 114–71 | - | - |
| Three-phase | PV | - | | 30 | |
| | SVC | 3,000 | | 52 | |
| | SOP | 6,000 | | 250-57 | |

### C. SIMULATION RESULTS

To verify the effectiveness of the proposed method, four scenarios were adopted, as follows:

- Base Scenario: The DSO did not have a voltage control scheme. No SVCs were installed, and no PVs were connected to the smart inverter. There was no change in the tap position of the tap changer;
- Scenario I: A local voltage control scheme was applied; voltage regulation devices (SVC and tap changer) determined the operating point by themselves to adjust **the voltage** at the connection point (i.e., secondary-side bus in the case of tap changer) as a reference value (1.0 p.u);
- Scenario II: The cooperative voltage control strategy of ANM was applied as represented in (23); SVC and tap changer were controlled to maximize the total HC for the PV;
- Scenario III: A power flow control device, defined as SOP [8], was added to improve the HC for the PV compared to that of Scenario II. The operating point of the SOP was included as the control variable for the cooperative voltage control strategy;
- Scenario IV: The volt-var curve parameter of the smart PV inverter was modified as shown in Table 2 to improve the HC for PV compared to that of Scenario III.

For a specific load profile in Scenario II, an example of calculating the correction variable by comparing the two profile curves (i.e., maximum available generation profile and actual PV profile) is shown in Fig. 7. From 11:00 to

**TABLE 2.** Volt-var curve parameters by scenarios.

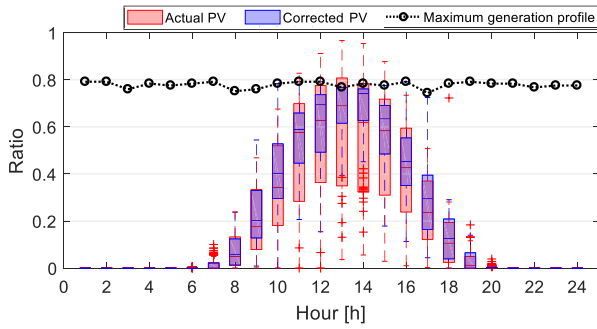| Parameters | Scenario I | Scenario II | Scenario III | Scenario IV |
|---|---|---|---|---|
| $V_{PCC,min}$ [p.u] | | 0.95 | | 0.98 |
| $V_{PCC,max}$ [p.u] | | 1.05 | | 1.02 |
| $V_{db,min}^{k}$ [p.u] | | 0.98 | | 0.99 |
| $V_{db,max}^{k}$ [p.u] | | 1.02 | | 1.01 |



**FIGURE 7.** Comparison before and after correction of actual PV profile curve.



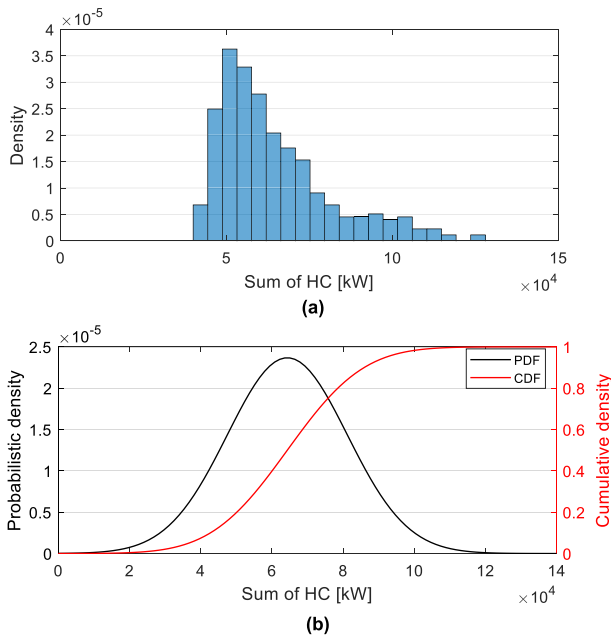**FIGURE 8.** Probability distribution of maximum HC for PV in Scenario II: (a) Histogram; (b) Probabilistic/Cumulative density function.



**FIGURE 9.** Comparison of probability distribution for maximum HC for PV between scenarios: (a) PDF; (b) CDF.

CDF of Fig. 8 (b), the HC value for a cumulative probability of 5% was 36,641 KW. This value means that if the DSO operates the DN with a PV penetration of 36,641 KW (as in Scenario II), the risk of violating the network reliability constraints is 5%.

The results of comparing the probability distributions for the maximum HC for the PV between scenarios are shown in Fig. 9. Several conclusions were drawn from the comparison results between each scenario as follows:

- From the comparison with Scenarios I and II, it can be concluded that more PV penetration can be secured if the DSO intervenes in the operation policy of the voltage regulation devices to perform cooperative control, rather than locally operating these devices;
- By comparing Scenarios II and III, it can be confirmed that power flow control using SOP has a positive effect on enhancing the HC. This is since active/reactive power flow control not only solves bottlenecks in the DN but also contributes to the voltage profiles of the nodes;
- The effects of the volt-var curve parameters of the smart PV inverter on the increase in HC can be obtained by comparing Scenarios III and IV. The steeper the slope of the volt-var curve, the more aggressive is the regulation of the reactive power output to maintain the voltage at the PV connection point. This reduced the sensitivity of the voltage rise relative to PV penetration. For the transition from Scenario III to IV, the DSO can notify each PV generator owner of a parameter change through regulations or recommendations. For DSO-owned PVs, an engineer directly dispatches to the location where the PV is installed and modifies the parameter.

Fig. 10 shows a boxplot comparison of the distribution of the maximum HC for each PV under different scenarios,

15:00, the network reliability constraints were violated in this horizon because the actual PV generation ratio (red box) was higher than the maximum available generation ratio (black line). Therefore, the maximum HC for the PV was determined by scaling down the PVBC (blue box) using the correction variable in (24).

Fig. 8 shows the probability distribution of the maximum HC for the PV for Scenario II. Using 50 loads and 100 PV profile curves, the maximum HC for PV for a total of 5,000 was calculated for each scenario. The probability distribution function (PDF) and cumulative distribution function (CDF) curves were generated by fitting the HC for PV data based on the Gaussian distribution function [41]. For instance, in the
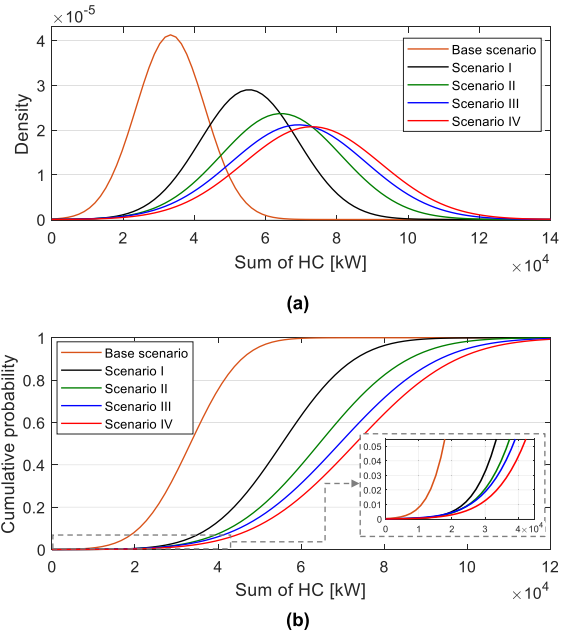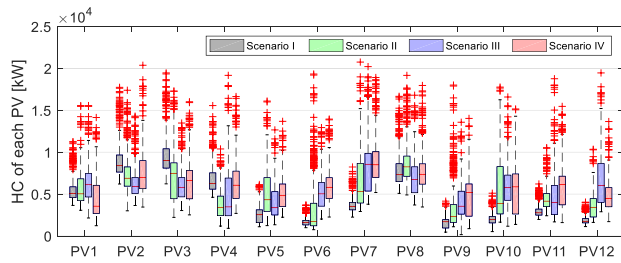
**FIGURE 10.** Boxplot comparison of each HC for PV between scenarios.

**TABLE 4.** Comparison of cumulative probability by HC.

| Cumulative Probability | | Scenario | | | | |
|---|---|---|---|---|---|---|
| | | Base | I | II | III | IV |
| Maximum HC for PV [kW] | 12,886 | 1.72% | 0% | 0% | 0% | 0% |
| | 23,391 | 15.18% | 1% | 0.75% | 0.75% | 0.49% |
| | 27,139 | 26% | 2% | 1.36% | 1.27% | 0.85% |
| | 29,518 | 34.66% | 3% | 1.93% | 1.75% | 1.18% |
| | 31,307 | 41.70% | 4% | 2.49% | 2.21% | 1.50% |
| | 32,763 | 47.65% | 5% | 3.04% | 2.64% | 1.81% |

which was determined to maximize the sum of HCs in the DN. Red cross marks in Fig. 10 are outliers in the box plot diagram, indicating the HC value at significantly lower or higher risk levels. If the DSO chooses the HC at the highest risk level (i.e., the red cross mark that corresponds to the highest HC value), there will be a high probability of violating constraints. As the network operation strategy of the DSO changes depending on the scenario, the optimal combination of PV capacity that maximizes the sum of HCs also varies. In Scenario I, because voltage regulation devices operate locally, the maximum capacity of individual PVs was not significantly affected by the volatility of PV generation and load demand. However, in the centralized ANM scheme (i.e., from Scenarios II to IV), the range of HC variation for each PV increased since the DSO directly controlled each device. Even in some PVs, the mean value in the distribution of HC was lower than in Scenario I. However, for the purpose of DSO, this sacrifice can be justified to maximize the sum of HCs within the DN. In other words, through the analysis of Fig. 10, the DSO can find out which scenario has the most impact on increasing the HC distribution at the target PV location. In addition, for the specific ANM strategy to be applied by the DSO, they can analyze the most effective candidates of PV location in terms of increase in the HC.

The numerical comparison results for the distribution of HC by scenario are shown in Tables 3 and 4. In Table 3, the maximum HCs are compared with respect to the specific risk (i.e., cumulative probability in Fig. 9), and values in parentheses indicate the incremental amount compared to the base scenario. Using the centralized ANM from DSO (i.e., Scenario II), additional PV installation up to approximately 3,878 KW is possible at a risk of 1% to 5% compared to local control (i.e., Scenario I). In addition, through the application of SOP and tuning the parameter of the smart PV inverter (i.e., Scenario IV), extra PV penetration of approximately 8,656 KW is possible, which means an improvement
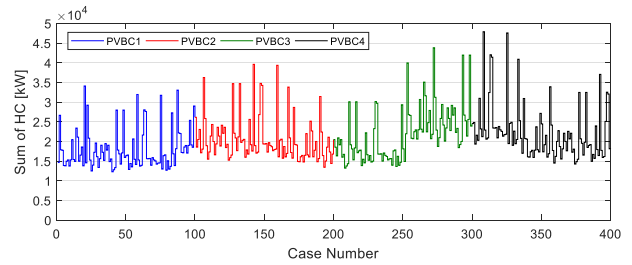


**FIGURE 11.** Example of the sum of HC regarding the PV profile cases

of about 26.4% (in 5% of the cumulative probability case). The risk values for the specific HC under each scenario are listed in Table 4. Under a constant PV penetration, the risk of violating network constraints can be reduced by up to 1.81% by utilizing the SOP and centralized control compared to Scenario I (in 32,763 KW of maximum HC for the PV case).

In this study, we used the global optimization solver (GA) to solve the co-simulation-based optimization framework linked with an external tool (OpenDSS). The computation time for simulation was about 46 minutes (2,772s). However, since the proposed framework is performed offline in the system planning stage, the computation time does not necessarily have to be significantly short. In addition, the setpoints calculated by the ANM are sent hourly to each controllable device but can be adjusted regarding the convenience of the DSO.

The HC has a unique value depending on the topology of the DN and where the DSO wants to install the PV. If the topology of the DN is changed, the DSO can recalculate the HC through the proposed method.

## IV. DISCUSSIONS
### A. RISK SELECTION
Through the risk figures calculated by this paper, the DSO should ultimately pick a proper risk value for determination of HC. At this time, the DSO can refer the reference values used in several previous studies; in [42], voltage violation condition of 3% in DN is targeted to control the distributed renewables. In China, the confidence constraint for the number of voltage fluctuations is limited using a probabilistic index such as 95% [43]. In South Korea, system operator defines the permissible value for the frequency of voltage fluctuations as its own reliability standards [44]. Besides, in the BS-EN-50160, 10-min voltage magnitudes should be within a specific range as a condition of 95% probability [45], [46]. However, the DSO can determine any new risk figures by analyzing the trade-offs between the risk of reliability violation and additional HC acquisition. For the DSO who wants to strict risk management, the proposed framework can be used as a deterministic way by applying specific representative PV and load profile curves (e.g., best and worst cases).

### B. PRACTICAL IMPLEMENTATION
After the DSO selects the sum of the HCs from the desired risk values, the DSO should check which PVBC set the

**TABLE 3.** Comparison of HC by cumulative probability.

| Additional HC for PV [kW] | | Base | Scenario | | | |
|---|---|---|---|---|---|---|
| | | | I | II | III | IV |
| Cumulative Probability | 0% | 8,435 (-) | 12,886 (+4,451) | 12,288 (+3,853) | 11,001 (+2,566) | 13,615 (+5,180) |
| | 1% | 10,846 (-) | 23,391 (+12,545) | 25,159 (+14,313) | 25,402 (+14,556) | 28,310 (+17,464) |
| | 2% | 13,481 (-) | 27,139 (+13,658) | 29,752 (+16,271) | 30,541 (+17,060) | 33,553 (+20,072) |
| | 3% | 15,153 (-) | 29,518 (+14,365) | 32,666 (+17,513) | 33,802 (+18,649) | 36,881 (+21,728) |
| | 4% | 16,410 (-) | 31,307 (+14,897) | 34,858 (+18,448) | 36,255 (+19,845) | 39,383 (+22,973) |
| | 5% | 17,433 (-) | 32,763 (+15,330) | 36,641 (+19,208) | 38,250 (+20,817) | 41,419 (+23,986) |

selected sum of HC belongs to. For example, Fig. 11 shows a plot of the sum of HC determined for 100 actual PV profiles. Four sets of representative PVBCs were calculated for the 4 load profile curves. If the sum of HC is selected as 12,500 KW, PVBC1 corresponds to the final base capacity, since the value of 12,500 KW belongs to the distribution of the sum of HC in PVBC1 as shown in Fig. 11. The final HC for each PV is then determined by multiplying the base capacity for each PV location by the correction variable ($\tau_s$) that corresponds to 12,500 KW.

If the selected value for the sum of HC is increased, intersections with multiple PVBC sets occur. For instance, if the value of 20,000 KW is selected as the sum of HC in Fig. 11, four sets of PVBCs correspond to the selected sum of HC. In this case, one PVBC set should be chosen according to the intent of the DSO. The DSO can consider other various factors, such as geographic conditions and the additional investment cost for the site.

## V. CONCLUSION

In this study, a two-stage optimization-based framework for determining the probabilistic HC for PV was proposed. The proposed method can reflect the probabilistic characteristics owing to the uncertainty of the PV and load output over time and quantify the improvement of the flexibility of the DN resulting from the integrated management of controllable resources by DSO. In addition, the benefit of a novel power controller called SOP was introduced to enhance the HC.

The proposed HC calculation framework allows the DSO to use the results of numerical analysis on the risk reduction effect by additional devices or network operation strategies to confirm the economic impact of new technologies. This can also be used to review whether the PV capacity to be installed is reasonable at a given location. In other words, the DSO can utilize the proposed method to calculate the sensitivity of the amount of additional HC for PV according to the introduction of new facilities or operation strategies in the grid planning stage and utilize them as a basis for their investment decision-making process.

Future research could include a process for determining the optimal location/rated capacity for a new facility or a new high-level cooperative operation strategy for the DSO to maximize the risk reduction impact on the HC for PV.

## REFERENCES

[1] (2020). IEA. *World Energy Outlook 2020*. International Energy Agency. Paris. [Online]. Available: https://www.iea.org/reports/world-energy-outlook-2020

[2] I. Konstantelos, S. Giannelos, and G. Strbac, "Strategic valuation of smart grid technology options in distribution networks," *IEEE Trans. Power Syst.*, vol. 32, no. 2, pp. 1293–1303, Mar. 2017.

[3] B. Palmintier, R. Broderick, B. Mather, M. Coddington, K. Baker, F. Ding, M. Reno, M. Lave, and A. Bharatkumar. On the Path to Sunshot: Emerging Issues and Challenges in Integrating Solar With the Distribution System. National Renewable Energy Laboratory. Accessed: May 2016. [Online]. Available: http://www.nrel.gov/docs/fy16osti/65331.pdf

[4] S. M. Ismael, S. H. E. A. Aleem, A. Y. Abdelaziz, and A. F. Zobaa, "State-of-the-art of hosting capacity in modern power systems with distributed generation," *Renew. Energy*, vol. 130, pp. 1002–1020, Jan. 2019.

[5] E. Mulenga, M. H. J. Bollen, and N. Etherden, "A review of hosting capacity quantification methods for photovoltaics in low-voltage distribution grids," *Int. J. Electr. Power Energy Syst.*, vol. 115, Feb. 2020, Art. no. 105445.

[6] K. M. Muttaqi, A. D. T. Le, M. Negnevitsky, and G. Ledwich, "A coordinated voltage control approach for coordination of OLTC, voltage regulator, and DG to regulate voltage in a distribution feeder," *IEEE Trans. Ind. Appl.*, vol. 51, no. 2, pp. 1239–1248, Apr. 2015.

[7] J. V. Milanovic and Y. Zhang, "Global voltage sag mitigation with FACTS-based devices," *IEEE Trans. Power Del.*, vol. 25, no. 4, pp. 2842–2850, Oct. 2010.

[8] P. Li, H. Ji, C. Wang, J. Zhao, G. Song, F. Ding, and J. Wu, "Optimal operation of soft open points in active distribution networks under three-phase unbalanced conditions," *IEEE Trans. Smart Grid*, vol. 10, no. 1, pp. 380–391, Jan. 2019.

[9] K. E. Antoniadou-Plytaria, I. N. Kouveliotis-Lysikatos, P. S. Georgilakis, and N. D. Hatziargyriou, "Distributed and decentralized voltage control of smart distribution networks: Models, methods, and future research," *IEEE Trans. Smart Grid*, vol. 8, no. 6, pp. 2999–3008, Nov. 2017.

[10] H. S. Bidgoli and T. Van Cutsem, "Combined local and centralized voltage control in active distribution networks," *IEEE Trans. Power Syst.*, vol. 33, no. 2, pp. 1374–1384, Mar. 2018.

[11] M. Juamperez, G. Yang, and S. B. Kjær, "Voltage regulation in LV grids by coordinated volt-var control strategies," *J. Modern Power Syst. Clean Energy*, vol. 2, no. 4, pp. 319–328, Dec. 2014.

[12] G. Yang, F. Marra, M. Juamperez, S. B. Kjær, S. Hashemi, J. Østergaard, H. H. Ipsen, and K. H. B. Frederiksen, "Voltage rise mitigation for solar PV integration at LV grids," *J. Modern Power Syst. Clean Energy*, vol. 3, no. 3, pp. 411–421, Sep. 2015.

[13] T. B. Rasmussen, G. Yang, A. H. Nielsen, and Z. Dong, "Effects of centralized and local PV plant control for voltage regulation in LV feeder based on cyber-physical simulations," *J. Modern Power Syst. Clean Energy*, vol. 6, no. 5, pp. 979–991, Sep. 2018.

[14] J. Hu, H. Zhou, Y. Li, P. Hou, and G. Yang, "Multi-time scale energy management strategy of aggregator characterized by photovoltaic generation and electric vehicles," *J. Modern Power Syst. Clean Energy*, vol. 8, no. 4, pp. 727–736, 2020.

[15] S. Wang, S. Chen, L. Ge, and L. Wu, "Distributed generation hosting capacity evaluation for distribution systems considering the robust optimal operation of OLTC and SVC," *IEEE Trans. Sustain. Energy*, vol. 7, no. 3, pp. 1111–1123, Jul. 2016.

[16] T. S. Ustun, J. Hashimoto, and K. Otani, "Impact of smart inverters on feeder hosting capacity of distribution networks," *IEEE Access*, vol. 7, pp. 163526–163536, 2019.

[17] F. Capitanescu, L. F. Ochoa, H. Margossian, and N. D. Hatziargyriou, "Assessing the potential of network reconfiguration to improve distributed generation hosting capacity in active distribution systems," *IEEE Trans. Power Syst.*, vol. 30, no. 1, pp. 346–356, Jan. 2015.

[18] M. S. S. Abad, J. Ma, D. Zhang, A. S. Ahmadyar, and H. Marzooghi, "Probabilistic assessment of hosting capacity in radial distribution systems," *IEEE Trans. Sustain. Energy*, vol. 9, no. 4, pp. 1935–1947, Oct. 2018.

[19] M. S. S. Abad and J. Ma, "Photovoltaic hosting capacity sensitivity to active distribution network management," *IEEE Trans. Power Syst.*, vol. 36, no. 1, pp. 107–117, Jan. 2021.

[20] F. Ding and B. Mather, "On distributed PV hosting capacity estimation, sensitivity study, and improvement," *IEEE Trans. Sustain. Energy*, vol. 8, no. 3, pp. 1010–1020, Jul. 2017.

[21] A. Arshad and M. Lehtonen, "A stochastic assessment of PV hosting capacity enhancement in distribution network utilizing voltage support techniques," *IEEE Access*, vol. 7, pp. 46461–46471, 2019.

[22] D. A. Quijano, J. Wang, M. R. Sarker, and A. Padilha-Feltrin, "Stochastic assessment of distributed generation hosting capacity and energy efficiency in active distribution networks," *IET Gener., Transmiss. Distrib.*, vol. 11, no. 18, pp. 4617–4625, Dec. 2017.

[23] H. Al-Saadi, R. Zivanovic, and S. F. Al-Sarawi, "Probabilistic hosting capacity for active distribution networks," *IEEE Trans. Ind. Informat.*, vol. 13, no. 5, pp. 2519–2532, Oct. 2017.

[24] B. Wang, C. Zhang, Z. Y. Dong, and X. Li, "Improving hosting capacity of unbalanced distribution networks via robust allocation of battery energy storage systems," *IEEE Trans. Power Syst.*, vol. 36, no. 3, pp. 2174–2185, May 2021.

[25] S. Taheri, M. Jalali, V. Kekatos, and L. Tong, "Fast probabilistic hosting capacity analysis for active distribution systems," *IEEE Trans. Smart Grid*, vol. 12, no. 3, pp. 2000–2012, May 2021.

[26] P. H. Divshali and L. Soder, "Improving hosting capacity of rooftop PVs by quadratic control of an LV-central BSS," *IEEE Trans. Smart Grid*, vol. 10, no. 1, pp. 919–927, Jan. 2019.

[27] X. Cao, T. Cao, F. Gao, and X. Guan, "Risk-averse storage planning for improving RES hosting capacity under uncertain siting choices" *IEEE Trans. Sustain. Energy*, vol. 12, no. 4, pp. 1984–1995, Oct. 2021.

[28] EPRI. *Simulation Tool—OpenDSS*. Accessed: Sep. 12, 2018. [Online]. Available: http://smart grid.epri.com/Simulation Tool.aspx

[29] V. C. Cunha, T. Kim, P. Siratarnsophon, N. Barry, S. Santoso, and W. Freitas, "Quasi-static time-series power flow solution for islanded and unbalanced three-phase microgrids," *IEEE Open Access J. Power Energy*, vol. 8, pp. 97–106, 2021.

[30] M. U. Qureshi, S. Grijalva, M. J. Reno, J. Deboever, X. Zhang, and R. J. Broderick, "A fast scalable quasi-static time series analysis method for PV impact studies using linear sensitivity model," *IEEE Trans. Sustain. Energy*, vol. 10, no. 1, pp. 301–310, Jan. 2019.

[31] J. Smith and M. Rylander, "'Stochastic analysis to determine feeder hosting capacity for distributed solar PV,'" Electr. Power Res. Inst., Palo Alto, CA, USA, Tech. Rep. 1026640, 2012, pp. 0885–8950.

[32] *IEEE Standard for Interconnection and Interoperability of Distributed Energy Resources with Associated Electric Power Systems Interfaces*, Standard 1547-2018, IEEE, Feb. 2018.

[33] California Energy Commission. *Rule 21 Smart Inverter Working Group Technical Reference Materials*. Accessed: Mar. 11, 2014. [Online]. Available: http://www.energy.ca.gov/electricity_analysis/rule21/

[34] D. Chathurangi, U. Jayatunga, S. Perera, A. P. Agalgaonkar, and T. Siyambalapitiya, "Comparative evaluation of solar PV hosting capacity enhancement using volt-VAr and volt-watt control strategies," *Renew. Energy*, vol. 177, pp. 1063–1075, Nov. 2021.

[35] N. E. M. Association, "American national standard for electric power systems and equipment-voltage ratings (60 hertz)," Nat. Elect. Manuf. Assoc., Rosslyn, VA, USA, Tech. Rep. ANSI C84.1-2006, Dec. 2006.

[36] A. Navarro-Espinosa and L. F. Ochoa, "Probabilistic impact assessment of low carbon technologies in LV distribution systems," *IEEE Trans. Power Syst.*, vol. 31, no. 3, pp. 2192–2203, May 2016.

[37] F. Braeuer, J. Rominger, R. McKenna, and W. Fichtner, "Battery storage systems: An economic model-based analysis of parallel revenue streams and general implications for industry," *Appl. Energy*, vol. 239, pp. 1424–1440, Apr. 2019.

[38] A. Hoke, R. Butler, J. Hambrick, and B. Kroposki, "Steady-state analysis of maximum photovoltaic penetration levels on typical distribution feeders," *IEEE Trans. Sustain. Energy*, vol. 4, no. 2, pp. 350–357, Apr. 2013.

[39] (2017). Distribution Test Feeders. *IEEE PES Distribution System Analysis Subcommittee*. [Online]. Available: http://ewh.ieee.org/soc/pes/dsacom/testfeeders/index.html

[40] S. Satsangi and G. B. Kumbhar, "Effect of load models on scheduling of VVC devices in a distribution network," *IET Gener., Transmiss. Distrib.*, vol. 12, no. 17, pp. 3993–4001, Sep. 2018.

[41] A. W. Bowman and A. Azzalini, *Applied Smoothing Techniques for Data Analysis*. New York, NY, USA: Oxford Univ. Press, 1997.

[42] Y. Jiang, C. Wan, J. Wang, Y. Song, and Z. Y. Dong, "Stochastic receding horizon control of active distribution networks with distributed renewables," *IEEE Trans. Power Syst.*, vol. 34, no. 2, pp. 1325–1341, Mar. 2019.

[43] F. Luo, W. Wei, C. Wang, J. Huang, Q. Yin, and Y. Bai, "Research and application of GIS-based medium-voltage distribution network comprehensive technical evaluation system," *Int. Trans. Electr. Energy Syst.*, vol. 25, no. 11, pp. 2674–2684, Nov. 2015.

[44] S. Kim, H. Kim, H. Lee, J. Lee, B. Lee, G. Jang, X. Lan, T. Kim, D. Jeon, Y. Kim, and J. Lee, "Expanding power systems in the Republic of Korea," *IEEE Power Energy Mag.*, vol. 17, no. 3, pp. 61–72, May/Jun. 2019.

[45] S. W. Alnaser and L. F. Ochoa, "Advanced network management systems: A risk-based AC OPF approach," *IEEE Trans. Power Syst.*, vol. 30, no. 1, pp. 409–418, Jan. 2015.

[46] Arrangement of Regulations, "The electricity safety, quality and continuity regulations 2002," Crown Copyright, U.K., 2002. [Online]. Available: https://www.centralpower.co.uk/admin/ckfinder/userfiles/files/ESQCR%202002.pdf

**CHANGHEE HAN** (Graduate Student Member, IEEE) received the B.S. and M.S. degrees in electrical engineering from Korea University, Seoul, South Korea, in 2015 and 2017, respectively, where he is currently pursuing the Ph.D. degree. He was a Research Engineer with Hyundai MOBIS Company Ltd., Yongin, South Korea, from 2017 to 2018. His research interests include optimization, MVDC distribution systems, and active distribution networks.

**DONGWON LEE** (Student Member, IEEE) received B.S. degree in electrical engineering from Korea University, Seoul, South Korea, in 2020, where he is currently pursuing the Ph.D. degree with the Department of Electrical Engineering. His research interests include optimization and control of distribution systems.

**SUNGYOON SONG** (Member, IEEE) received the B.S. degree in electrical engineering from Soongsil University, in 2015, and the M.S. and Ph.D. degrees in electrical engineering from Korea University, Seoul, South Korea, in 2020. From 2020 to 2021, he was a Senior Researcher with the Korea Institute of Energy Research (KIER), Daejeon, South Korea. He is currently a Senior Researcher with the Korea Electrotechnology Research Institute (KERI), Uiwang-si, South Korea. His research interests include modeling and control of VSC-HVDC, FACTS, and reinforcement learning application.

**GILSOO JANG** (Senior Member, IEEE) received the B.S. and M.S. degrees from Korea University, Republic of Korea, and the Ph.D. degree from Iowa State University, Ames, IA, USA, in 1997. He worked as a Visiting Scientist at the Department of Electrical and Computer Engineering, Iowa State University, for one year, and a Researcher at the Korea Electric Power Research Institute, for two years. He is currently a Professor at the School of Electrical Engineering, Korea University. His research interests include power system dynamics and control.

● ● ●